Science Advances
AAAS

advances.sciencemag.org/cgi/content/full/5/4/eaau6547/DC1

Supplementary Materials for

Helicobacter pylori–induced matrix metallopeptidase-10 promotes gastric bacterial colonization and gastritis

Yi-pin Lv, Ping Cheng, Jin-yu Zhang, Fang-yuan Mao, Yong-sheng Teng, Yu-gang Liu, Hui Kong, Xiao-long Wu, Chuan-jie Hao, Bin Han, Qiang Ma, Shi-ming Yang, Weisan Chen, Liu-sheng Peng, Ting-ting Wang, Quan-ming Zou, Yuan Zhuang*

*Corresponding author. Email: yuanzhuang1983@yahoo.com

Published 3 April 2019, *Sci. Adv.* **5**, eaau6547 (2019)
DOI: 10.1126/sciadv.aau6547

This PDF file includes:

Supplementary Figures

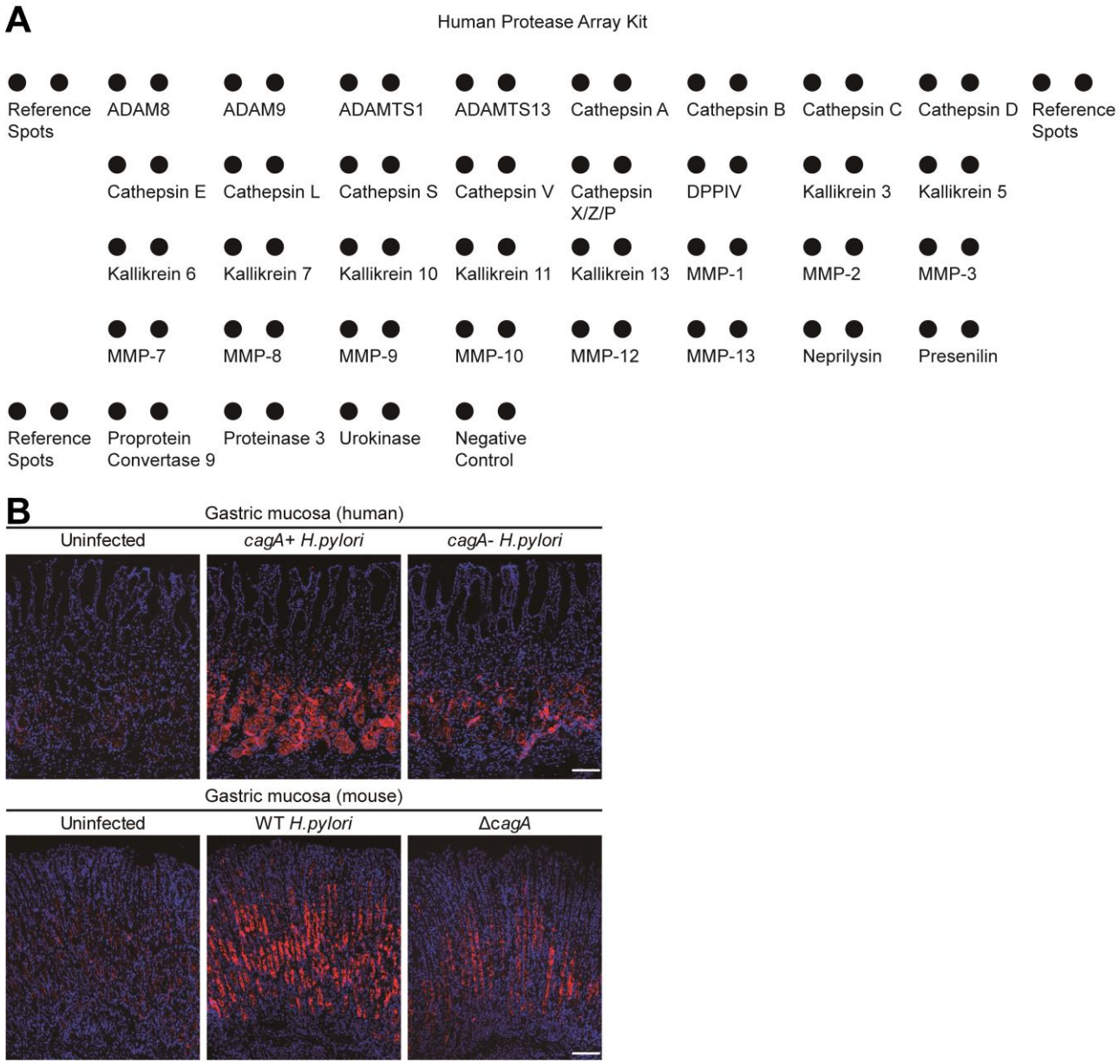

Fig. S1. MMP-10 is increased in gastric mucosa of *H. pylori*–infected patients and mice. (**A**) Refer to the image for the Human Protease Array coordinates. (**B**) MMP-10 protein in gastric mucosa of *cagA*$^{+}$*H. pylori*-infected, *cagA*$^{-}$*H. pylori*-infected, and uninfected donors or in gastric mucosa of WT *H. pylori*-infected, *ΔcagA*-infected, and uninfected mice at 9 week p.i. was analyzed by immunofluorescence staining. Scale bars: 100 microns. * P<0.05, ** P<0.01 for groups compared with uninfected mice.

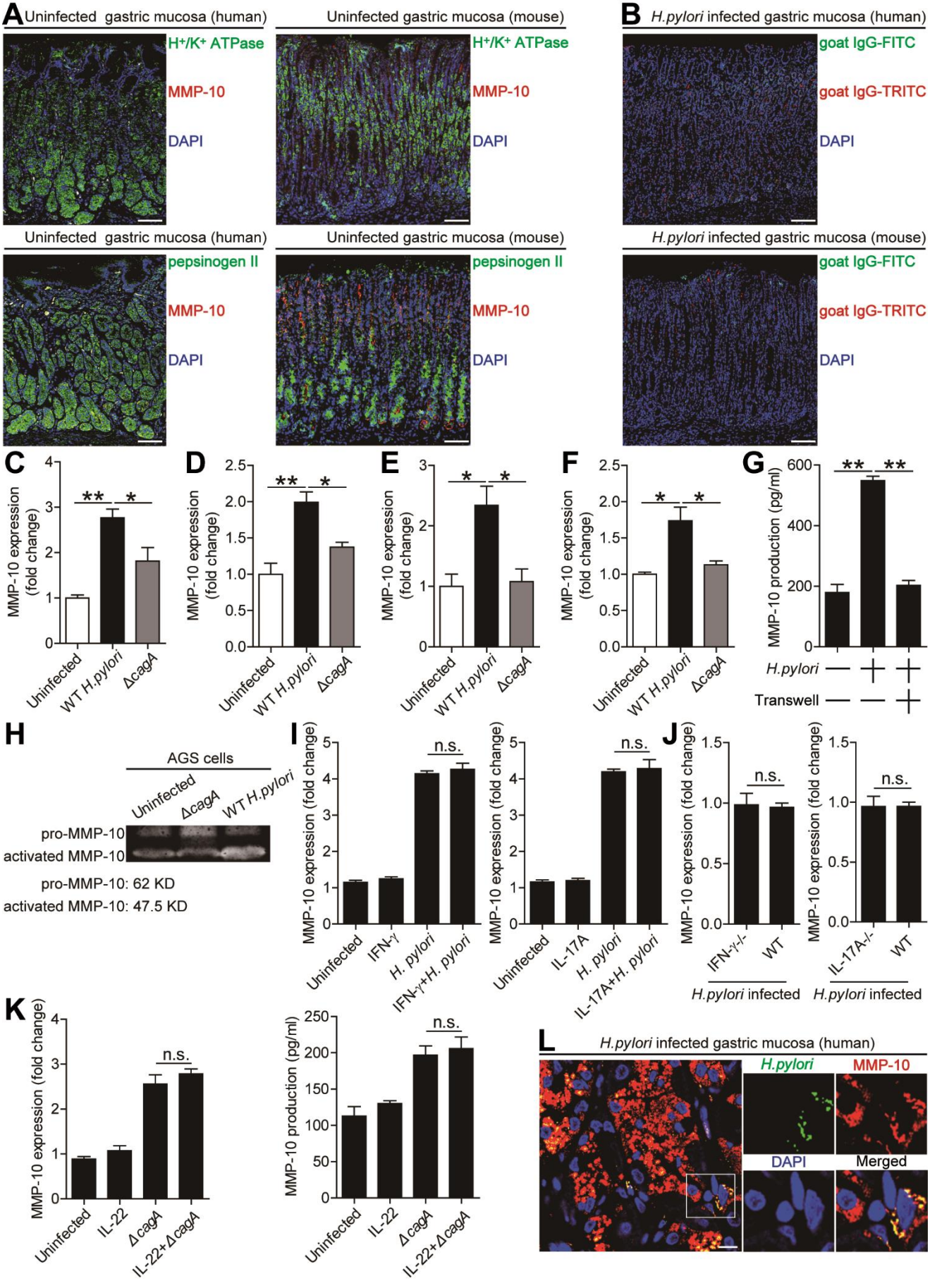

Fig. S2. *H. pylori* and IL-22 synergistically induce gastric epithelial cells to express MMP-10.

(**A**) Representative immunofluorescence staining images showing MMP-10-expressing (red) H^+/K^+ $ATPase^+$ parietal cells (green) and MMP-10-expressing (red) pepsinogen II^+ chief cells (green) in gastric mucosa of uninfected donors or uninfected mice. Scale bars: 100 microns. (**B**) Representative immunofluorescence staining images showing only secondary antibody staining controls in gastric mucosa of *H. pylori*-infected patients or *H. pylori*-infected mice. Scale bars: 100 microns. (**C**-**F**) MMP-10 mRNA expression in WT *H. pylori*-infected, *ΔcagA*-infected, and uninfected GES-1 cells (C), BGC-823 cells (D), HGC-27 cells (E), and SGC-7901 cells (F) (MOI=100, 24 h) was analyzed by real-time PCR (n=3). (**G**) The induction of MMP-10 production from AGS cells infected with WT *H. pylori* (MOI=100, 24 h) was assessed by transwell assay and analyzed by ELISA (n=3) as described in Materials and Methods. (**H**) Activated MMP-10 from AGS cells infected with WT *H. pylori* or *ΔcagA* (MOI=100, 24 h) was assessed by casein-zymography assay as described in Materials and Methods. (**I**) MMP-10 mRNA expression in AGS cells stimulated with WT *H. pylori* (MOI=100) and/or IFN-γ, or IL-17A (100 ng/ml) (24 h) was analyzed by real-time PCR (n=3). (**J**) MMP-10 mRNA expression in gastric mucosa of WT *H. pylori*-infected WT, $IFN\text{-}\gamma^{-/-}$, or $IL\text{-}17A^{-/-}$ mice at 9 week p.i.was compared (n=5). (**K**) MMP-10 mRNA expression and MMP-10 protein in/from AGS cells stimulated with *ΔcagA* (MOI=100) and/or IL-22 (100 ng/ml) (24 h) was analyzed by real-time PCR and ELISA (n=3).(**L**) Representative immunofluorescence staining images showing MMP-10-expressing (red) cells and *H. pylori* (green) colonization in gastric mucosa of *H. pylori*-infected patients. Scale bars: 10 microns.* $P<0.05$, ** $P<0.01$, n.s. $P>0.05$ for groups connected by horizontal lines.

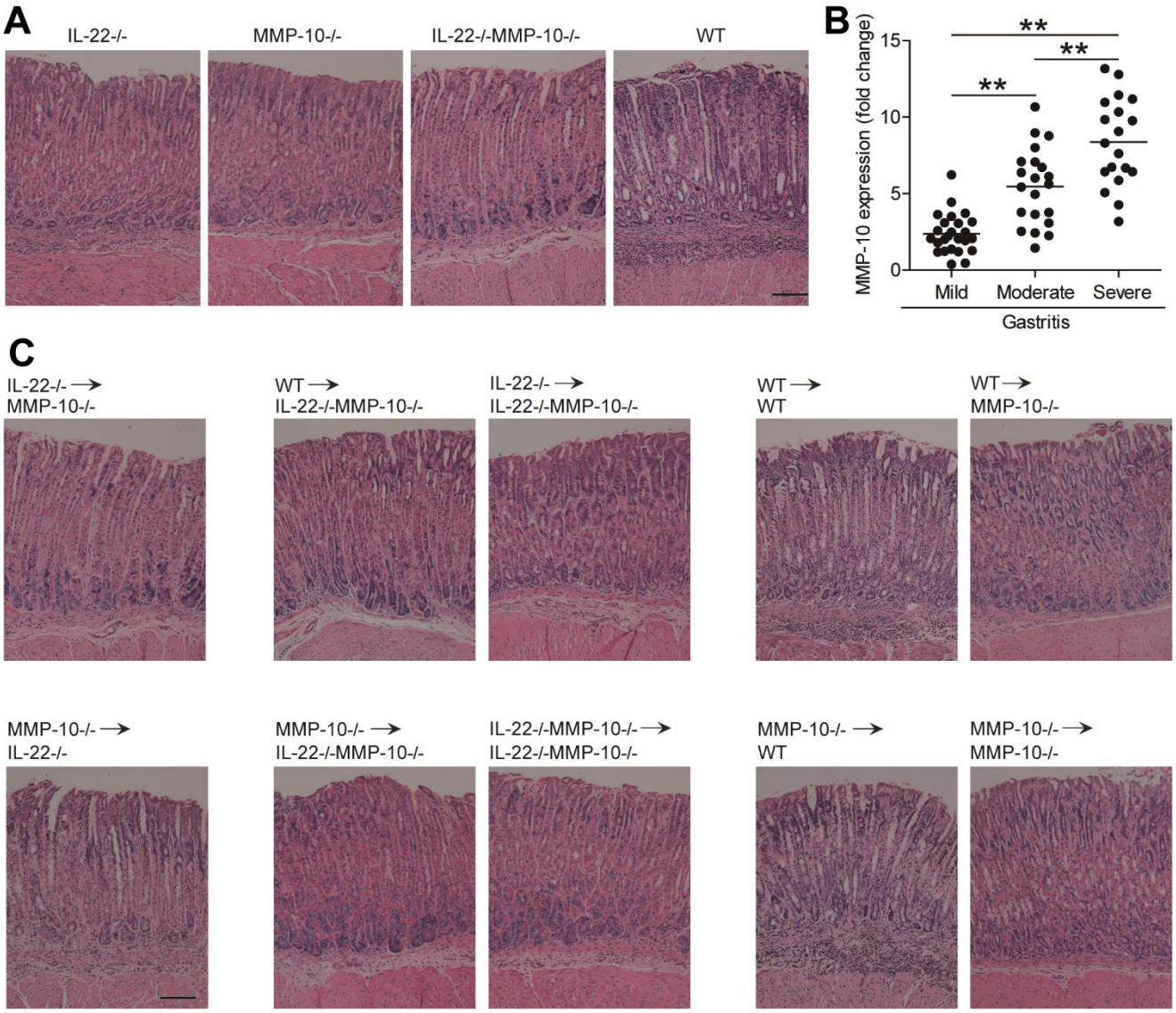

Fig. S3. MMP-10 increases bacterial burden and inflammation in gastric mucosa during *H. pylori* infection. (**A**) Representative H&E staining images showed inflammation in gastric antra of WT *H. pylori*-infected IL-22$^{-/-}$, MMP-10$^{-/-}$, IL-22$^{-/-}$MMP-10$^{-/-}$, and WT mice at 9 week p.i.. Scale bars: 100 microns. (**B**) MMP-10 mRNA expression in gastric mucosa of *H. pylori*-infected patients with mild (n=25), moderate (n=20), and severe inflammation (n=19) was compared. (**C**) Representative H&E staining images showed inflammation in gastric antra of WT *H. pylori*-infected BM chimera mice at 9 week p.i.. Scale bars: 100 microns. The horizontal bars in panel B represent mean values. Each dot in panel B represents 1 patient. ** P<0.01 for groups connected by horizontal lines.

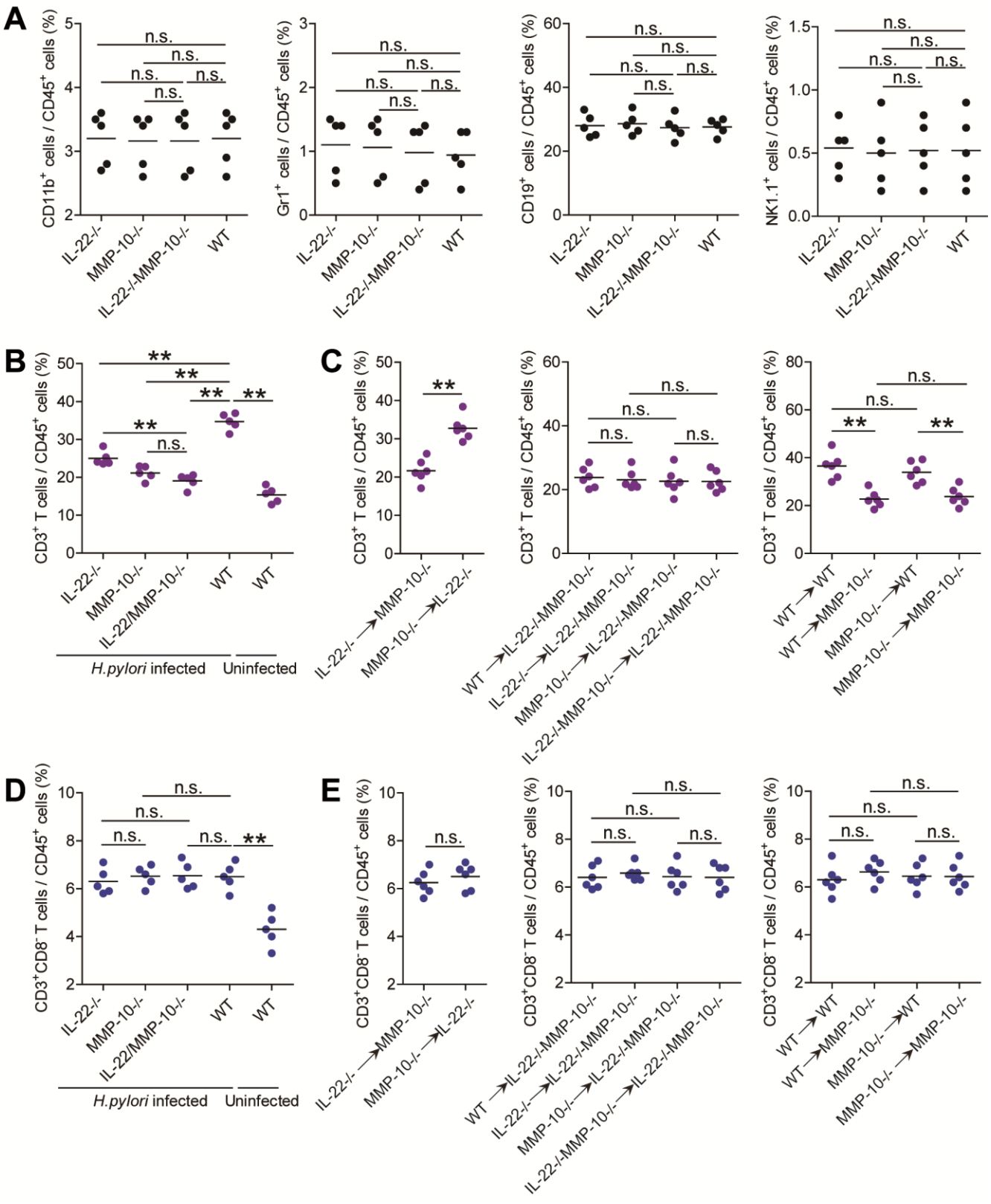

Fig. S4. MMP-10 promotes CD8⁺ T cell accumulation in gastric mucosa in vivo during *H. pylori* infection. (**A**) The levels of CD11b⁺ monocytes, Gr1⁺ neutrophils, CD3⁺ T cells, CD19⁺ B cells, and NK1.1⁺ natural killer cells (NK cells)in gastric mucosa of WT *H. pylori*-infected IL-22$^{-/-}$, MMP-10$^{-/-}$, IL-22$^{-/-}$MMP-10$^{-/-}$, and WT mice at 9 week p.i. were compared (n=5). (**B**) CD3⁺cell level in

gastric mucosa of uninfected WT mice, and WT *H. pylori*-infected IL-22$^{-/-}$, MMP-10$^{-/-}$, IL-22$^{-/-}$MMP-10$^{-/-}$, and WT mice at 9 week p.i. was compared (n=5). (**C**) CD3^{+} cell level in gastric mucosa of WT *H. pylori*-infected BM chimera mice at 9 week p.i. was compared (n=6). (**D**) CD3^{+}CD8^{-} cell level in gastric mucosa of uninfected WT mice, and WT *H. pylori*-infected IL-22$^{-/-}$, MMP-10$^{-/-}$, IL-22$^{-/-}$MMP-10$^{-/-}$, and WT mice at 9 week p.i. was compared (n=5). (**E**) CD3^{+}CD8^{-} cell level in gastric mucosa of WT *H. pylori*-infected BM chimera mice at 9 week p.i. was compared (n=6). The horizontal bars in panel A, B, C, D, and E represent mean values. Each dot in panel A, B, C, D, and E represents 1 mouse. ** P<0.01, n.s. P>0.05 for groups connected by horizontal lines.

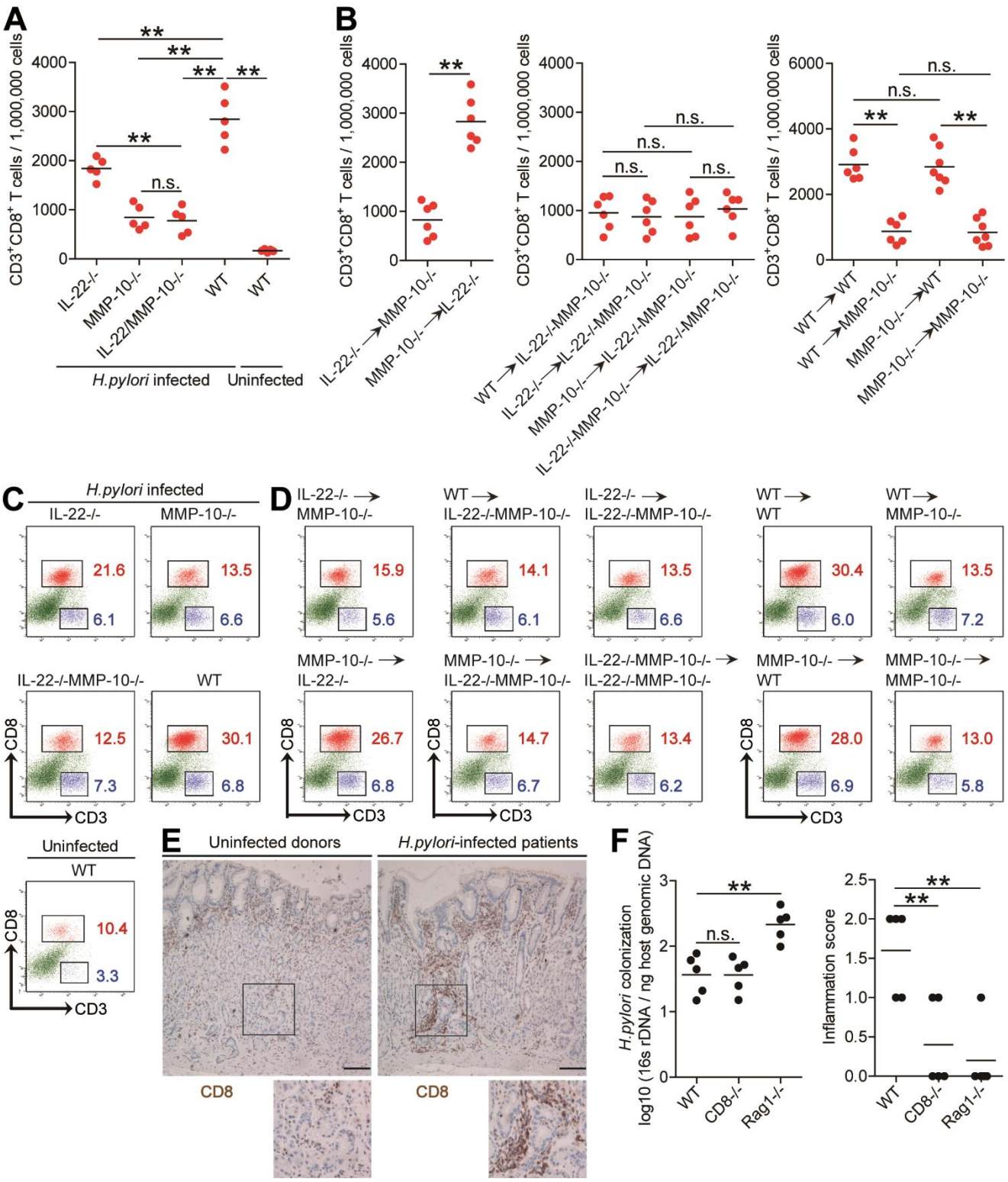

Fig. S5. MMP-10 promotes CD8⁺ T cell accumulation in gastric mucosa in vivo during *H. pylori* infection. (**A**) $CD3^+CD8^+$ cell number in gastric mucosa of uninfected WT mice, and WT *H. pylori*-infected IL-$22^{-/-}$, MMP-$10^{-/-}$, IL-$22^{-/-}$MMP-$10^{-/-}$, and WT mice at 9 week p.i. was compared (n=5). (**B**) $CD3^+CD8^+$ cell number in gastric mucosa of WT *H. pylori*-infected BM chimera mice at 9 week p.i. was compared (n=6). (**C**) Representative dot plots of $CD3^+CD8^+$ cells by gating on $CD45^+$ cells

in gastric mucosa of uninfected WT mice, and WT *H. pylori*-infected IL-22$^{-/-}$, MMP-10$^{-/-}$, IL-22$^{-/-}$MMP-10$^{-/-}$, and WT mice at 9 week p.i.. Red or blue numbers indicate relative percentages of CD3^{+}CD8^{+} cells or CD3^{+}CD8^{-} cells in CD45^{+} cells. (**D**) Representative dot plots of CD3^{+}CD8^{+} cells by gating on CD45^{+} cells in gastric mucosa of WT *H. pylori*-infected BM chimera mice at 9 week p.i.. Red or blue numbers indicate relative percentages of CD3^{+}CD8^{+} cells or CD3^{+}CD8^{-} cells in CD45^{+} cells. (**E**) CD8^{+} T cell infiltration in gastric mucosa of uninfected donors and *H. pylori*-infected patients was analyzed by immunohistochemical staining. Scale bars: 100 microns. (**F**) The bacteria colonization and the histological scores of inflammation in gastric mucosa of WT *H. pylori*-infected CD8$^{-/-}$, Rag1$^{-/-}$, and WT mice at 9 week p.i. were compared (n=5). The horizontal bars in panel A, B and F represent mean values. Each dot in panel A, B and F represents 1 mouse. * $P<0.05$, ** $P<0.01$, n.s. $P>0.05$ for groups connected by horizontal lines.

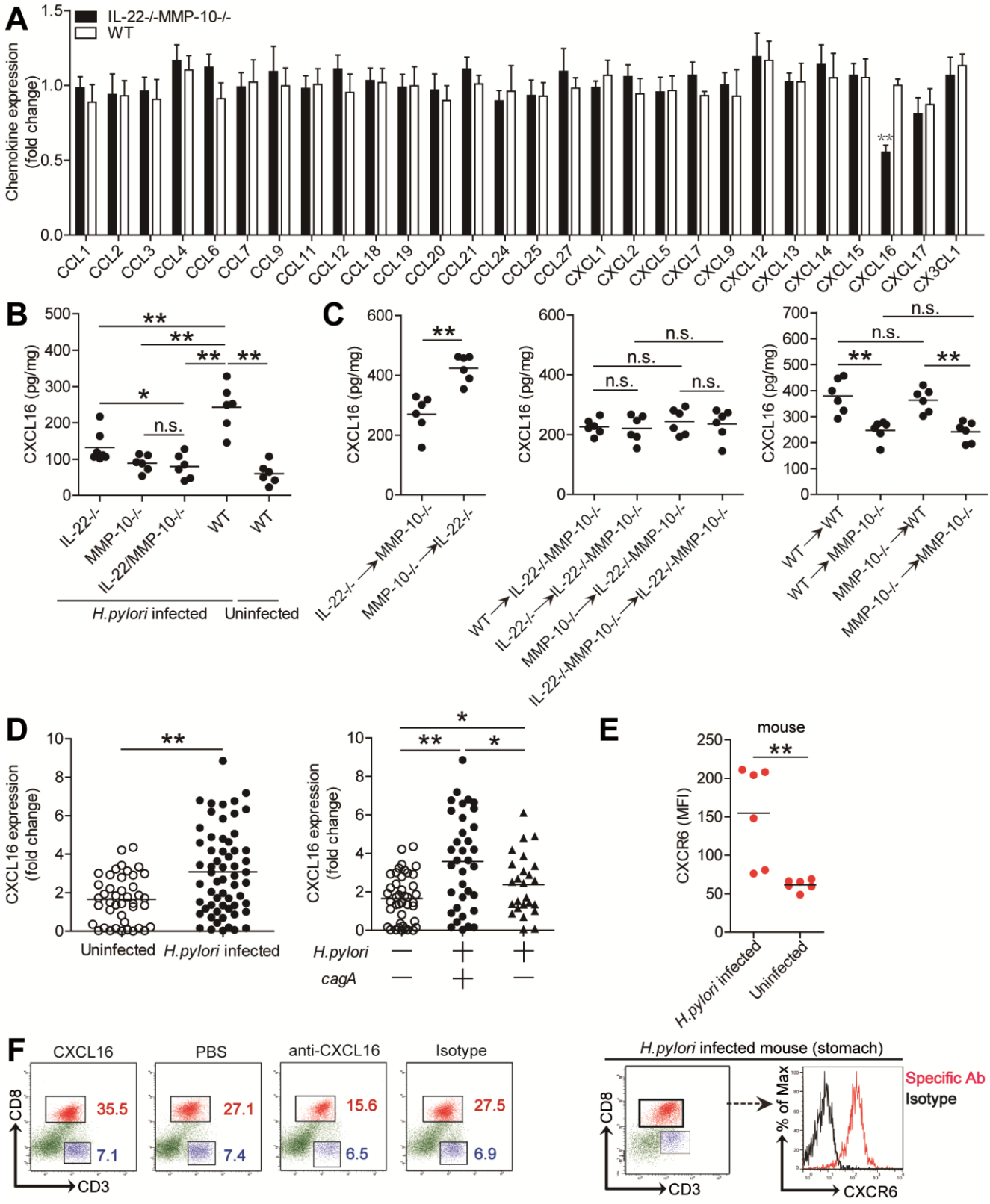

Fig. S6. MMP-10 promotes CD8$^+$ T cell accumulation in gastric mucosa in vivo and migration in vitro during *H. pylori* infection by CXCL16. (**A**) Chemokine mRNA expression in gastric mucosa of WT *H. pylori*-infected IL-22$^{-/-}$MMP-10$^{-/-}$ and WT mice at 9 week p.i. was compared (n=5).(**B** and **C**) Concentrations of CXCL16 protein in gastric mucosa of uninfected WT mice, and

WT *H. pylori*-infected IL-22$^{-/-}$, MMP-10$^{-/-}$, IL-22$^{-/-}$MMP-10$^{-/-}$, and WT mice (B), or in gastric mucosa of WT *H. pylori*-infected BM chimera mice (C) at 9 week p.i. was compared (n=6). (**D**) CXCL16 mRNA expression in gastric mucosa of *H. pylori*-infected (n=62) and uninfected donors (n=42) was compared.CXCL16 mRNA expression in gastric mucosa of *cagA*$^{+}$*H. pylori*-infected (n=35), *cagA*$^{-}$*H. pylori*-infected (n=25),and uninfected donors (n=42) was compared. (**E**) Representative dot plots of CD3^{+}CD8^{+} cells by gating on CD45^{+} cells, and CXCR6 expression on CD3^{+}CD8^{+} cells in stomach of WT *H. pylori*-infected mice at 9 week p.i.. CXCR6 levels on CD3^{+}CD8^{+} cells in stomach of WT *H. pylori*-infected and uninfected mice at 9 week p.i. were compared (n=6). (**F**) Representative dot plots of CD3^{+}CD8^{+} cells by gating on CD45^{+} cells in gastric mucosa of WT *H. pylori*-infected WT mice injected with CXCL16 or PBS control, or Abs against CXCL16 or corresponding isotype control Ab at 9 week p.i.. Red or blue numbers indicate relative percentages of CD3^{+}CD8^{+} cells or CD3^{+}CD8^{-} cells in CD45^{+} cells. The horizontal bars in panel B, C, D and E represent mean values. Each dot or ring in panel B, C, D and E represents 1 donor or mouse. * P<0.05, ** P<0.01, n.s. P>0.05 for groups connected by horizontal lines, or compared with WT mice.

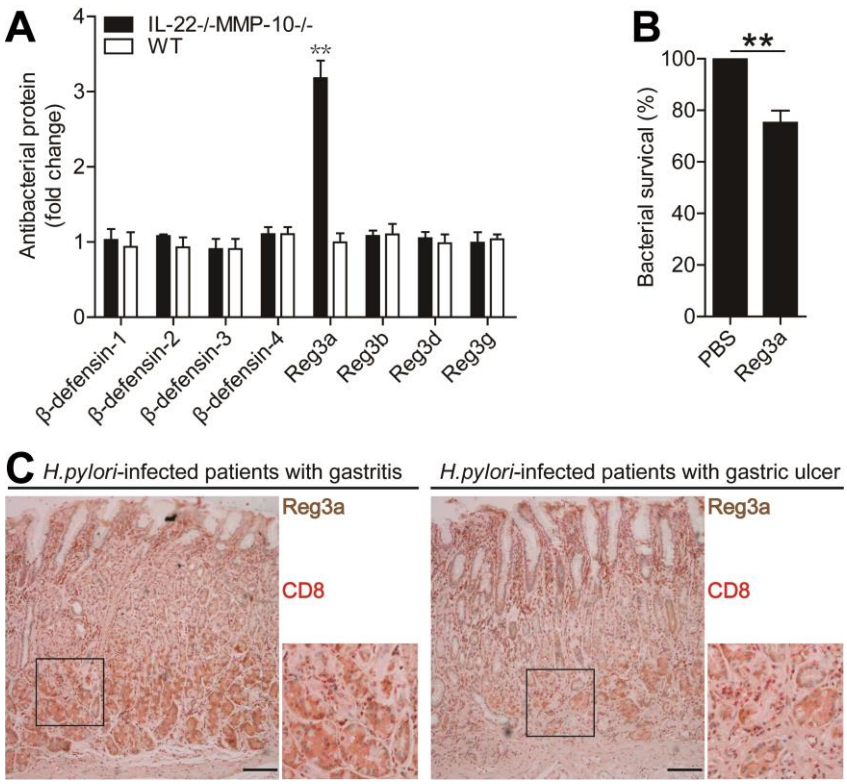

Fig. S7. MMP-10 impairs host defense and promotes the damage of gastric mucosa during *H. pylori* infection. (**A**) The mRNA expression of β-defensins and Reg3 proteins in gastric mucosa of

WT *H. pylori*-infected IL-22$^{-/-}$MMP-10$^{-/-}$ and WT mice at 9 week p.i. was compared (n=5). (**B**) *In vitro* bactericidal assay was performed as described in Methods and statistically analyzed (n=5). The results was determined by counting colony-forming units (CFU) of alive bacteria with agar plating and expressed as the survival rate of WT *H. pylori* after incubation with Reg3a or PBS. (**C**) The Reg3a expression and CD8^{+} T cell infiltration in gastric mucosa of *H.pylori*-infected patients with gastritis or gastric ulcer was analyzed by immunohistochemical staining. Scale bars: 100 microns. ** P<0.01 for groups connected by horizontal lines, or compared with WT mice.

Table S1. Clinical characteristics of patients.

Variables	*H. pylori*-infected	Uninfected
Age (median, range)	(45 year, 20–72 years)	(47 year, 25–69 years)
Sex (male/female)	55/41	22/20

Exclusion criteria were: previous treatment for *H. pylori* infection, use of inhibitors of acid secretion and/or antibiotics during the 2 months before the study, use of anticoagulant drugs in the last week, gastrointestinal malignancy, severe concomitant cardiovascular, respiratory or endocrine diseases, clinically significant renal or hepatic disease, haematological disorders, previous gastro-oesophageal surgery, history of allergy to any of the drug used in the study, pregnancy or lactation, alcohol abuse, drug addiction, severe neurological or psychiatric disorders, and long-term use of corticosteroids or anti-inflammatory drugs.

Table S2. Antibodies and other reagents.

Antibodies and reagents	Manufacturers
Antibodies for flow cytometry	
anti-mouse CD45-PE-Cy7	Biolegend
anti-mouse CD3-APC	Biolegend
anti-mouse CD8-PerCP-Cy5.5	Biolegend
anti-mouse CD11b-PerCP-Cy5.5	Biolegend
anti-mouse Gr1-FITC	Biolegend
anti-mouse CD19-APC-Cy7	Biolegend
anti-mouse NK1.1-PE	Biolegend
anti-mouse CXCR6-FITC	Biolegend
anti-human CD45-PE-Cy7	Biolegend
anti-human CD3-APC	Biolegend
anti-human CD8-PerCP-Cy5.5	Biolegend
anti-human CXCR6-FITC	Biolegend
Antibodies for immunohistochemical staining	
rabbit anti-human/mouse MMP-10	Abcam
horseradish peroxidase anti-rabbit IgG	Zhongshan Biotechnology
mouse anti-human CD8	Abcam
rabbit anti-human Reg3a	Raybiotech
Polymer Double Dyeing Detection Kit (Mo/HRP+Rb/AP)	Zhongshan Biotechnology
Antibodies for immunofluorescence	
rabbit anti-human/mouse MMP-10	Abcam
mouse anti-human/mouse H^+/K^+ ATPase	Abcam
rabbit anti-human/mouse pepsinogen II	Santa Cruz
rabbit anti-*H. pylori*	Raybiotech
goat anti-rabbit-TRITC	Zhongshan Biotechnology
goat anti-rabbit-FITC	Zhongshan Biotechnology
goat anti-mouse-TRITC	Zhongshan Biotechnology
goat anti-mouse-FITC	Zhongshan Biotechnology
Antibodies for neutralizing and blocking	
anti-human CXCL16 (Rat IgG2a)	R&D Systems
anti-mouse CXCL16 (Rat IgG2a)	R&D Systems
Rat IgG2a Isotype Control	R&D Systems
anti-human IL-22 (Goat IgG)	R&D Systems
anti-human IL-22 receptor alpha 1 (Goat IgG)	R&D Systems
Goat IgG Control	R&D Systems
anti-mouse Reg3a (Rat IgG2a)	Santa Cruz

Rat IgG2a Isotype Control	Santa Cruz
Antibodies for western blot	
rabbit anti-human/mouseMMP-10	Abcam
rabbit anti-human ERK1/2	Cell signaling technology
rabbit anti-human p-ERK1/2	Cell signaling technology
rabbit anti-human/mouse GAPDH	Beijing Ray Antibody Biotech
mouse anti-mouse E-cadherin	Abcam
rabbit anti-mouse zonula occludens-1	Abcam
ELISA kits	
humanMMP-10	Raybiotech
human CXCL16	Raybiotech
mouse CXCL16	Raybiotech
mouse Reg3a	CUSABIO
Reagents for signaling pathways inhibition	
MEK-1 and MEK-2 inhibitorU0126	Merk Millipore
IκBαinhibitor BAY 11-7082	Calbiochem
JNK inhibitor SP600125	Calbiochem
MAPK inhibitor SB203580	Calbiochem
GSK-3β inhibitor VI	Calbiochem
Human CD326 microbeads	MilteniyBiotec
Mouse CD326 microbeads	MilteniyBiotec
5-μm pore size Transwells	Corning
0.4-μm pore size Transwells	Corning
Collagenase IV	Gibco
DNaseI	Sigma-Aldrich
DMSO	Sigma-Aldrich
Protein Extraction Reagent	Pierce
SuperSignal® West Dura Extended Duration Substrate kit	Thermo
Fetal bovine serum (FBS)	Gibco
Penicillin/Streptomycin	Gibco
RPMI-1640	Hyclone
DMEM/F12 (1:1)	Hyclone
Ficoll-Paque Plus	GE Healthcare
lyses solution	TIANGEN
TRIzol reagent	Invitrogen
Lipofectamine™ 3000 Transfection Reagent	Invitrogen

QIAamp DNA Mini Kit	QIAGEN
PrimeScriptTM RT reagent Kit	TaKaRa
Real-time PCR Master Mix	Toyobo
Proteome Profiler Human Protease Array Kit	R&D Systems
Casein-zymography	GENMED
Recombinant mouse Reg3a	R&D Systems
Recombinant human Reg3a	R&D Systems
All recombinant human/mouse cytokines and chemokines	PeproTech

APC-Cy7, allophycocyanin-cyanin 7; PE-Cy7, phycoerythrin-cyanin 7; FITC, Fluorescein isothiocyanate; PE, phycoerythrin; PerCP-Cy5.5, peridinchlorophyl protein-cyanin 5.5; APC, allophycocyanin; IL, interleukin.

Table S3. Primer and probe sequences for real-time PCR analysis.

Gene	Primer or probe	Sequence 5′→3′
H. pylori 16s rDNA	forward	TTTGTTAGAGAAGATAATGACGGTATCTAAC
	reverse	CATAGGATTTCACACCTGACTGACTATC
	probe	CGTGCCAGCAGCCGCGGT
Mouse β2-microglobulin	forward	CCTGCAGAGTTAAGCATGCCAG
	reverse	TGCTTGATCACATGTCTCGATCC
	probe	TGGCCGAGCCCAAGACCGTCTAC
H. pylori cagA	forward	GAGTCATAATGGCATAGAACCTGAA
	reverse	TTGTGCAAGAAATTCCATGAAA
Mouse Sry	forward	TGGGACTGGTGACAATTGTC
	reverse	GAGTACAGGTGTGCAGCTCT
Human GAPDH	forward	ACCCAGAAGACTGTGGATGG
	reverse	CAGTGAGCTTCCCGTTCAG
Mouse β-actin	forward	AGTGTGACGTTGACATCCGT
	reverse	GCAGCTCAGTAACAGTCCGC
Human IL-22	forward	GACAAGTCCAACTTCCAG
	reverse	GCTCACTCATACTGACTC
Human MMP-10	forward	GCTCTTTCACTCAGCCAACA
	reverse	TGCCATTCACATCATCTTGC
Mouse MMP-10	forward	CCTGTGTTGTCTGTCTCTCCAAGA
	reverse	CGTGCTGACTGAATCAAAGGA
Mouse CCL1	forward	ATGGCACTGATGTGCCTGCT
	reverse	GGTGGAGGACTGAGGGAAA
Mouse CCL2	forward	TCACCTGCTGCTACTCATTCA
	reverse	CACTGTCACACTGGTCACTCC
Mouse CCL3	forward	TTCTCTGTACCATGACACTCTGC

	reverse	CGTGGAATCTTCCGGCTGTAG
Mouse CCL4	forward	TGTCTGCCCTCTCTCTCCTCT
	reverse	AGCAAGGACGCTTCTCAGTGA
Mouse CCL5	forward	GCTGCTTTGCCTACCTCTCC
	reverse	TCGAGTGACAAACACGACTGC
Mouse CCL6	forward	CCAAGACTGCCATTTCATTC
	reverse	AAGCAATGACCTTGTTCCCA
Mouse CCL7	forward	ATGGAAGTCTGCGCTGAAG
	reverse	ACATGAGGTCTCCAGAGCTTT
Mouse CCL8	forward	ACGCTAGCCTTCACTCCAAAA
	reverse	TTCCAGCTTTGGCTGTCTCTT
Mouse CCL9	forward	TGGCATATCTGGCTTTGTCA
	reverse	ATGGCTGTAGCTCAAGATGGT
Mouse CCL11	forward	TCCACAGCGCTTCTATTCCT
	reverse	GCAGTTCTTAGGCTCTGGGTT
Mouse CCL12	forward	TCGAAGTCTTTGACCTCAACA
	reverse	GGGAACTTCAGGGGGAAATA
Mouse CCL19	forward	ACTTGCACTTGGCTCCTGAA
	reverse	AGTCTTCCGCATCATTAGCA
Mouse CCL20	forward	GCAAGCGTCTGCTCTTCCTT
	reverse	TTAGGCTGAGGAGGTTCACA
Mouse CCL21	forward	GATGATGACTCTGAGCCTCCT
	reverse	TTCTGCACCCAGCCTTCCT

Mouse CCL22	forward	TGGCAATTCAGACCTCTGATG
	reverse	TTGCTGGAATGGCAGAAGAA
Mouse CCL24	forward	TCATCTTGCTGCACGTCCTTT
	reverse	TAAACCTCGGTGCTATTGCCA
Mouse CCL25	forward	TCTCAGGACCAGAAAGGCATT
	reverse	TGGCGGAAGTAGAATCTCACA
Mouse CCL27	forward	AGGCTGAGTGAGCATGATGGA
	reverse	TTGGCGTTCTAACCACCGA
Mouse CCL28	forward	GCTGTGTGTGTGGCTTTTCAA
	reverse	TACCTCTGAGGCTCTCATCCA
Mouse CX3CL1	forward	TGGCTTTGCTCATCCGCTATCAG
	reverse	CGTCTGTGCTGTGTCGTCTCC
Mouse CXCL1	forward	ACCCAAACCGAAGTCATAG
	reverse	TTGTATAGTGTTGTCAGAAGC
Mouse CXCL2	forward	ACTTCAAGAACATCCAGAG
	reverse	CTTTCCAGGTCAGTTAGC
Mouse CXCL3	forward	CAGCCACACTCCAGCCTA
	reverse	CACAACAGCCCCTGTAGC
Mouse CXCL4	forward	AGCGATGGAGATCTTAGCTGTGT
	reverse	CCAGGCTGGTGATGTGCTTAA
Mouse CXCL5	forward	AGTCAAGAATCATTGGTTGTTAACCTT
	reverse	TCCGGAGACAATGCAATAGTCA
Mouse CXCL7	forward	GGAGTTCACTGTGCTGATGTGGA

	reverse	CACAGATGAAGCAGCTGGTCAGTAA
Mouse CXCL9	forward	ACAAATCCCTCAAAGACCTCAAACAG
	reverse	ATCTCCGTTCTTCAGTGTAGCAATG
Mouse CXCL10	forward	TGAAAGCGTTTAGCCAAAAAAGG
	reverse	AGGGGAGTGATGGAGAGAGG
Mouse CXCL12	forward	CCTCCAAACGCATGCTTCA
	reverse	ACTCTCCTCCCTTCCATTGCA
Mouse CXCL13	forward	CAGGCCACGGTATTCTGGA
	reverse	CAGGGGGCGTAACTTGAATC
Mouse CXCL14	forward	GCTTCATCAAGTGGTACAAT
	reverse	CTGGCCTGGAGTTTTTCTTTCCAT
Mouse CXCL15	forward	CTAGGCATCTTCGTCCGTCC
	reverse	TTGGGCCAACAGTAGCCTTC
Mouse CXCL16	forward	AAACATTTGCCTCAAGCCAGT
	reverse	GTTTCTCATTTGCCTCAGCCT
Mouse CXCL17	forward	ATGAAGCTTCTAGCCTCTCCC
	reverse	CTATAAGGGCAGCGCAAAGCTTGC
Mouse BD-1	forward	GAACACGGTACACAGGCTTCC
	reverse	CCTGAATCACAGATGTCCAAG
Mouse BD-2	forward	CTCTCTGGAGTCTGAGTGCCC
	reverse	AGGACGCCTGGCAGAAGGAGG
Mouse BD-3	forward	TGCTGCTGTCTCCACCTGC
	reverse	AGTGTTGCCAATGCACCGAT

Mouse BD-4	forward	ACATGCATGACCAATGGAGCC
	reverse	CATCTTGCTGGTTCTTC
Mouse Reg3a	forward	CTGCTCTCCTGCCTGTTGTT
	reverse	GGAGCGATAAGCCTTGTAACC
Mouse Reg3b	forward	AGGCTTATGGCTCCTACTGCT
	reverse	GAAGCCTCAGCGCTATTGAG
Mouse Reg3g	forward	TGCCTATGGCTCCTATTGCT
	reverse	CATGGAGGACAGGAAGGAAG
Mouse Reg3d	forward	CTGTCTTCTCCACGCATCAG
	reverse	CTGCTCCACTTCCATCCATT

For the probes, a FAM fluorescent reporter is coupled to the 5' end, and a TAMRA quencher is coupled to the 3' end. BD, β-defensin.